Proceedings of the Combustion Institute, Volume 29, 2002/pp. 2343–2349

A FULLY INTEGRATED KINETIC MONTE CARLO/MOLECULAR DYNAMICS APPROACH FOR THE SIMULATION OF SOOT PRECURSOR GROWTH

A. VIOLI,[1] A. KUBOTA,[2] T. N. TRUONG,[3] W. J. PITZ,[2] C. K. WESTBROOK[2] AND A. F. SAROFIM[1]

[1]*Department of Chemical and Fuels Engineering*
University of Utah
Salt Lake City, UT 84112, USA
[2]*Lawrence Livermore National Laboratories*
Livermore, CA 94551, USA
[3]*Henry Eyring Center for Theoretical Chemistry*
Department of Chemistry
University of Utah
Salt Lake City, UT 84112, USA

The emphasis in this paper is on presenting a new methodology, together with some illustrative applications, for the study of polycyclic aromatic hydrocarbon polymerization leading to soot, widely recognized as a very important and challenging combustion problem. The new code, named fully integrated Kinetic Monte Carlo/Molecular Dynamics (KMC/MD), places the two simulation procedures on an equal footing and involves alternating between KMC and MD steps during the simulation. The KMC/MD simulations are used in conjunction with high-level quantum chemical calculations. With traditional kinetic rates and dealing with the growth of particles, it is often necessary to perform a lumping procedure in which much atomic-scale information is lost. Our KMC/MD approach is designed to preserve atomic-scale structure: a single particle evolves in time with real three-dimensional structure (bonds, bond angles, dihedral angles). In this paper, the methodology is illustrated by a sample simulation of high molecular mass compound growth in an environment (T, H, H_2, naphthalene, and acenaphthylene concentrations) of a low-pressure laminar premixed benzene/oxygen/argon flame with an equivalence ratio of 1.8. The use of this approach enables the investigation of the physical (e.g., porosity, density, sphericity) as well as chemical (e.g., H/C, aromatic moieties, number of cross-links) properties.

Introduction

This paper is directed at the development of a new tool for examining the molecular transformations that occur in combustion conditions during the transition from gas-phase precursors to soot particles. Although the H-abstraction-carbon-addition pathway for soot formation is well established, there is increasing evidence for a parallel polymerization pathway [1–7]. Recently, we developed a kinetic mechanism in which high molecular mass aromatic compounds are postulated to form by the reactive polymerization of small polycyclic aromatic hydrocarbons (PAH) [4,8–10]. The mechanism involves a sequence of chemical reactions between aromatic compounds with six π-electrons (e.g., benzene, naphthalene) and compounds containing conjugated double bonds (e.g., acenaphthylene, cyclopentadiene, indene). The distinguishing features of this mechanism and its importance in explaining experimental observations are reported elsewhere [9]. The acetylene addition and polymerization routes for soot formation probably occur in parallel in relative amounts that depend on the fuel and the combustion conditions. The polymerization reactions are frequently expressed in generalized global terms such as $A_i + A_j = A_{i+j}$. Recently, several papers have addressed the chemical details of the elementary steps for this global polymerization reaction [9,10].

The main thrust of this article is to provide the missing microscopic detail of the molecule growth, which is experimentally inaccessible, using large-scale, statistical mechanics simulations and molecular dynamics, in conjunction with high-level quantum chemical calculations. The strength of this approach is that it provides information on the physical as well as chemical structure of soot precursors, providing long-term potential for information on particle characteristics such as density, porosity, and other physical properties.

After summarizing in the following section the methodological details of the computations performed, we will provide results from the quantum chemical calculations and from the use of the fully integrated Kinetic Monte Carlo/Molecular Dynamics (KMC/MD) code.

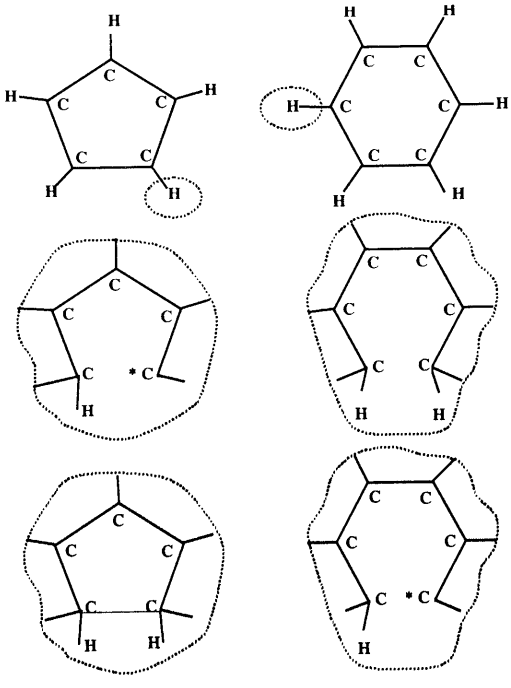

FIG. 1. Reaction sites defined in the KMC/MD code.

Method

The fully integrated KMC/MD method here proposed combines the strengths of two common simulation methods: KMC [11] and MD [12,13]. This feature represents the peculiarity of the new proposed methodology; the two approaches have been widely used [14–16], but have never been integrated in this way. The combination of the two techniques spans two time- and equilibrium scales: MD allows for relaxation as well as processes very far from equilibrium, while the KMC part allows much larger timescale changes to the system, provided that the system is at equilibrium. The time step for a single KMC iteration is a "real time," determined by the kinetics system.

The result is a rapidly convergent method, which is able to solve the sampling problem with many organic molecules and complexes. The reaction rates among the compounds present in the system are specified as probabilities, and the surface configuration over time is then given by a master equation, describing the time evolution of the probability distribution of system configurations.

Structure Simulation

Simulation parameters

There are three basic modules that determine the evolution of the structure. They are (1) the reaction site module, (2) the gas-phase module, and (3) the kinetic rate expression module.

1. The reaction site module governs the definition and counting algorithm of reaction sites, which are capable of undergoing modification (for example, addition reactions). Reaction sites have been defined in the context of the empirical bond-order potentials of Brenner [17], which are able to capture many of the essential features of chemical bonding in hydrocarbons. The analytical function is a highly parametrized version of Tersoff's empirical-bond-order formalism [18]. Non-local effects have been incorporated via an analytic function that defines conjugation based on the coordination of carbon atoms that neighbor carbon-carbon bonds. Because only nearest-neighbor interactions are incorporated, the function is very quickly evaluated and can therefore be used in large-scale MD simulations. The following sites have been defined in this study: (1) H atom on a five-membered ring, (2) H atom on a six-membered ring, (3) dangling bond on a five-membered ring, (4) dangling bond on a six-membered ring, (5) sp^3 hydrogen, (6) HCCCCR chains prone to close to form five-membered rings, (7) HCCCCCR chains prone to close to form six-membered rings, (8) HCCCCCH chains prone to close to form five-membered rings, and (9) HCCCCCCH chains prone to close to form six-membered rings. In the chains, R is a radical carbon. Examples of these sites are shown in Fig. 1. Bonding pairs are defined according to the formalism of Brenner. Hence, chains and rings are identified through efficient nested loops directed by neighbor list pointers. Additional proximity and geometric conditions are placed on the definition of the HC–CH chains to ensure that false-positive sites are not identified. Proximity conditions are also placed on radical sites. In the site-counting procedure, a radical carbon is considered as a possible site for termination or addition by a gas-phase species only if the gas-phase species of interest can be accommodated.

2. In the gas-phase module, the user must define the number of different gas-phase species and their concentrations in the environment.

3. The third module driving the particle evolution is the kinetic rate constant module. Reactions and kinetic rate constants are introduced as a function of time, temperature, pressure, and molecular weight. The configurations are stochastically integrated according to the kinetics we provide. A transition event is selected randomly, with its weight proportional to its kinetic rate. This rate for a typical gas-surface reaction is

$$r = kC_g N_s \tag{1}$$

where k is the pressure- and temperature-dependent rate constant, C_g is the gas-phase concentration, and N_s is the surface-site density or number for a particular reaction in which gas-species g reacts with a

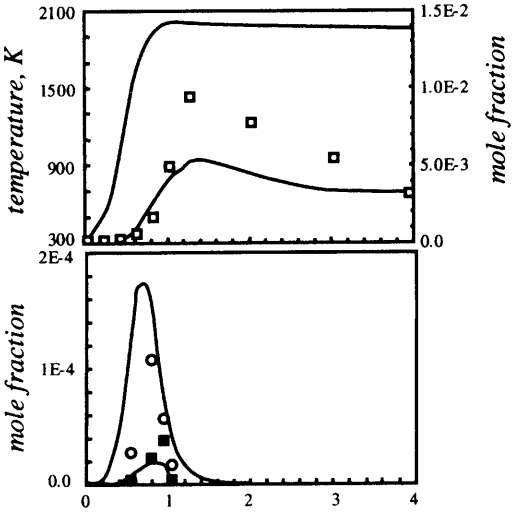

FIG. 2. Comparison between the computed concentration profiles of naphthalene, acenaphthylene, and H and experimental data for a C_6H_6 low-pressure flame [29].

particular surface site s. The real structure of a compound is decomposed into one that is defined by an array of surface positions.

Algorithmic approach

The modification to the particle is determined by the solution to the Master equation, which is given in equation 2,

$$\frac{dP_\alpha}{dt} = \sum_\beta (W_{\beta\to\alpha}P_\beta - W_{\alpha\to\beta}P_\alpha) \qquad (2)$$

where $P_\alpha(P_\beta)$ is the probability of finding the system in configuration $\alpha(\beta)$, and the W's are transition probabilities per unit time for various reactions [19]. The weighted transition probabilities are given as the normalized rates of all possible reactions/transitions calculated using the three modules discussed previously. Once the reaction and reaction site are determined, the structure is modified appropriately. For H-abstraction reactions here, hydrogen atoms are simply removed from the list of existing atoms, and the particle is then subjected to relaxation for 2 ps using the molecular dynamics module. Ring-closure reactions to form five- and six-membered rings involve a longer procedure, in which the C-C distance between the ends of the chain are gradually brought together, while all other atoms are allowed to relax. We have found reliable results by using increments of 5×10^{-6} Å for closing the rings. After the ring has been closed, full relaxation is performed for 2 ps. At this point, the molecule is ready for the next iteration, in which the reaction sites of the new updated particle are counted.

The new methodology can be expressed as follows:

Configuration 1 → (KMC) → Configuration 2
Configuration 2 → (MD) → Configuration 3
Configuration 3 → (KMC) → Configuration 4

Each iteration in the MD-KMC code goes as follows:

1. Take gas-phase concentrations (typically from the user or another application)
2. Perform site-counting procedure: identify every atom with a local environment which fits the definition of each site and check if there is enough room next to the site for a gas-phase specie to penetrate and react
3. Evaluate the kinetic rate constants ($k = AT^n \exp(-E_a/RT)$) and the reaction rates ($r = kC_gN_s$) (the kinetics have been calculated through electronic structure calculations; see next section)
4. Select reaction with probability proportional to its rate
5. Randomly select the first site for the reaction chosen
6. Perform modification of site according to the reaction transition (move a H for abstraction, add some species, etc.)
7. Perform energy minimization

Reaction Kinetics

Kinetic parameters for the possible reactions among the species present in the systems have been evaluated using the Transition State Theory (TST) [20], and the Evans-Polanyi linear free-energy formula [21] within the reaction-class TST formalism, to provide activation energies of reactions in a given reaction class. The potential energy information were calculated using the hybrid density functional Becke's three-parameter non local exchange function (B3LYP) method (i.e., B3LYP/6-31G(d,p) [22–24]), that represents the highest level of theory we could use given the size of the molecules and the current computational capability. The accuracy of this method has been reported by several research groups [25–27]. All calculations have been performed by using the Gaussian 98 program [28].

Conditions

High molecular mass compound growth is modeled in the environment of a low-pressure (2.67 kPa) laminar premixed C_6H_6/O_2/Ar flame of Bittner and Howard [29] with an equivalence ratio of 1.8. Temperature profile and H, H_2, naphthalene, and acenapthylene concentrations are used as input to the KMC/MD code. The profiles have been calculated using the CHEMKIN package [30] together with a kinetic model previously developed [31], and the computed results are compared with the experimental data in Fig. 2. The choice of the input PAH is due to their presence in high concentrations in the

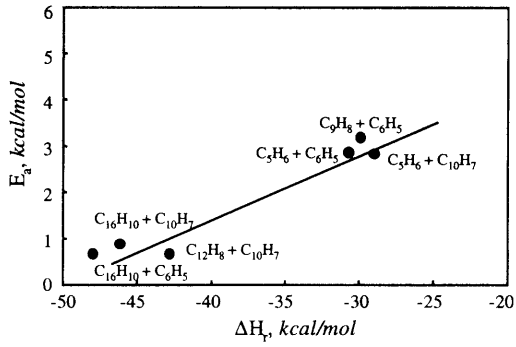

FIG. 3. Activation barriers versus the heat of reaction for a number of propagation step reactions. The data show the relation for the addition of phenyl and naphthyl radicals to the class of cyclopentafused hydrocarbons.

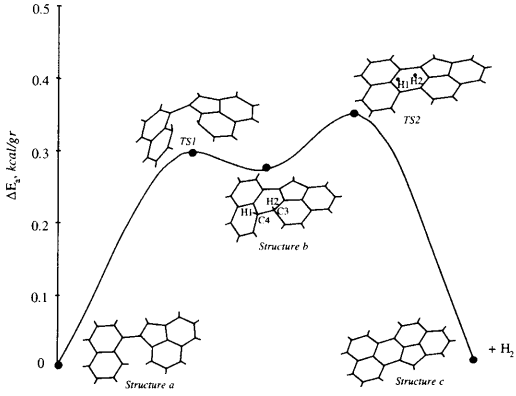

FIG. 4. Relative energy ΔE (kcal/gr) diagram for ring closure and dehydrogenation involving H1 and H2 from structure *a* obtained through the addition of 1-naphthyl to acenaphthylene.

PAH inventory and to the importance that PAH with peripherally fused five-membered rings (CP-PAH), which include acenaphthylene, have in the flame formation chemistry of soot [32–38] and fullerenes [39]. In using these concentrations in the KMC/MD code, no allowance was made in the calculated PAH and H profiles for species depletion or temperature change.

We decided to start our simulation from a temperature of 1400 K, that corresponds to the distance from the burner where the signal from species larger than 200 amu appears in the reference flame [29].

Results and Discussion

Results using Quantum Chemical Approach

The sequence for aromatic growth begins with the H abstraction from aromatic compounds to produce the corresponding radical [9], that furnishes higher aromatics through a two-step radical-molecule propagation step that involves addition reactions. Iteration of this mechanism followed by rearrangement of the carbon framework ultimately leads to the formation of high molecular mass compounds [4,10].

The Evans–Polanyi linear free-energy formula [40] was used to derive the activation energies in a given reaction class. H-abstraction reaction rates for the reaction of acenaphthylene, cyclopenta[*cd*]-pyrene, anthracene, and pyrene to form the corresponding radical and H_2 are reported elsewhere [41]. Fig. 3 reports the relation for another class of reaction that includes the addition of a radical to the double bonds of cyclopenta-fused PAH, for example, phenyl and naphthyl radical addition to cyclopentadiene, acenaphthylene, and aceanthrylene. The results obtained show agreement with the Hammond postulate: as the reactions become more exothermic, the energetic barriers are lower and shifted toward the reactants. Using this approach, it is possible to derive a relationship between the activation barriers and the heat of reaction for several reactions belonging to the same class.

As input information for the kinetic rate expression module to the KMC/MD code, we also added reaction rates for ring closure. The same type of analysis was done for the addition reactions, it has been applied to the ring-closure chemistry, namely, cyclodehydrogenation reactions, that leads to the increased extension of aromatic islands inside the structure. As an example of these calculations, we report in Fig. 4 the energy profile for ring closure and dehydrogenation involving H1 and H2 for structure *a* obtained by the addition of 1-naphthyl to the double bond of acenaphthylene. Through a first transition state (TS1), a bond is formed between C3 and C4 that brings to the formation of a six-membered ring (structure b). The ring closure is endothermic by ca. 2.86×10^{-1} kcal/g. The connection between (TS1)-Structure *b*-(TS2) is confirmed by intrinsic reaction coordinate calculations. From structure *b*, the reaction continues by elimination of H_2. The atoms H1 and H2 are now both in the same plane, and their distance of separation is 1.9 Å. In the final configuration, structure *c*, the two H atoms have been eliminated. More details about this type of reaction are reported elsewhere [41,42].

Results using Hybrid Monte Carlo Method

The results obtained through density functional theory (DFT) calculations in terms of reaction rates have been plugged into the KMC/MD code. Starting from a gas-phase bulk containing acenaphthylene, naphthalene, H_2, and H, the calculations follow the growth of an individual substrate (in this case naphthalene) to which compounds from the bulk are added. A transition event is selected randomly, with

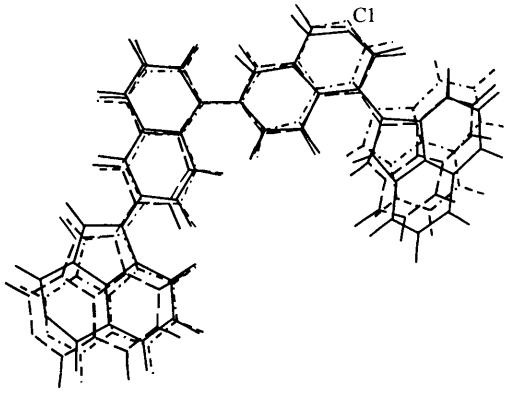

FIG. 5. Modifications that occur during the MD calculations for the intermediate $C_{44}H_{24}$.

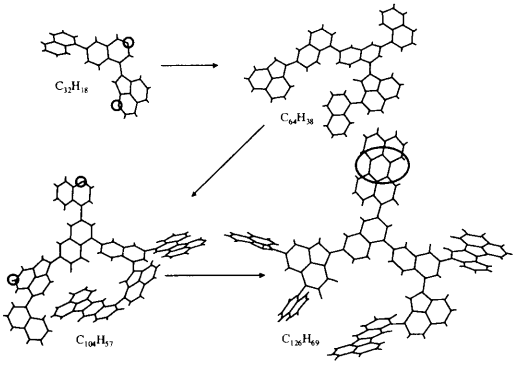

FIG. 6. Structural evolutions of high molecular mass compounds using the KMC/MD code.

its weight proportional to its kinetic rate. KMC/MD allows sampling long timescales, where the time duration between Monte Carlo events can be arbitrarily long (depending on the kinetics, model, etc.), while in MD, we require time steps that are a small fraction of the atomic vibrational period. MD allows for relaxation, while the KMC part allows much larger timescale changes to the system.

In order to better describe the methodology and to highlight the importance of MD in this method, we analyze the $C_{44}H_{24}$ compound reported in Fig. 5. It represents an intermediate produced during the molecular growth process, and it was obtained from $C_{44}H_{25}$ through H abstraction from C1. In this case, the hydrogen atom is simply removed from the list of existing atoms, and the particle is then subjected to relaxation for a few picoseconds using the MD module, that allows the structure to reach a relaxed local minimum. Fig. 5 shows the changes that occur to the structure during the first 2 ps of relaxation (dashed line, after 1 ps; solid line, after 2 ps). The calculations on molecular configurations can provide information on the proximity of H atoms and the probable sites for ring closure.

After the application of the MD, new potential reactions and reaction sites are identified, and the KMC module is applied for a given interval to calculate the new structures formed. Examples of structural evolutions of high molecular mass compounds are shown in Fig. 6 for the system selected (the starting compound is naphthalene).

Structure 2 ($C_{64}H_{38}$) is formed from structure 1 through H abstraction and further addition of two molecules of naphthalene and one of acenaphthylene. The addition sites for the compounds are highlighted to help the reader. After further H abstraction and naphthalene addition, structure 3 ($C_{104}H_{57}$) is produced. Structure 4 has a formula of $C_{126}H_{69}$, and a ring-closure reaction has occurred (the site is evidenced).

The introduction of ring-closure reactions by dehydrogenation in the kinetic scheme allows the formation of curved structures. The H/C ratio of the structures slowly decreases, going from 0.57 for the first structure to 0.53 for the last in the present limited simulation. Ultimately, further dehydrogenation reactions lead to the carbon nanoparticles such as soot and fullerenes. Evidence for molecules such as those shown in Fig. 6 is provided by Homann and coworkers [43], who analyzed large PAH molecules and radicals in a low-pressure benzene oxygen flame (C/O = 0.8, v = 42 cm s^{-1}, P = 2.66 kPa), using molecular beam time-of-flight mass spectrometry combined with resonance-enhanced multiphoton ionization. They reported a C-H diagram for each molecular formula C_xH_y identified in flame for PAH and PAH radicals. The combination of the polymerization mechanism together with the KMC/MD code allow us to build compounds with H/C ratios in the range identified by the authors and to provide information on the chemical structure. For example, the compounds $C_{32}H_{18}$, and $C_{44}H_{24}$ produced by the code have H/C ratios of soot precursors in the range identified by Homann and coworkers [43] and that are much higher than those of polybenzenoid structures of equal molecular weight.

A larger number of simulations can give statistical information about the system, that is, H/C and molecular weight distribution, moieties, and cross-linking characteristics as function of time.

Discussion and Conclusions

In this paper, we have presented a new code that combines the strengths of KMC and MD methods. This code, named fully integrated KMC/MD, represents a new tool for the study of the transformations that occur during soot formation. The use of this methodology allows sampling on long timescales, where the time-duration between Monte

Carlo events can be arbitrarily long (depending on the kinetics, model, etc), while MD simulations require a time step that is a small fraction of the atomic vibrational period. The features of the two methods have been illustrated with detailed examples.

To shed light on the mechanism of hydrocarbon growth, the fully-integrated KMC/MD code in conjunction with high-level quantum chemical calculations was used to carry out simulations for the formation of soot precursor structures. The environment chosen for this analysis is a low-pressure laminar premixed benzene/oxygen/argon flame studied by Bittner and Howard [29]. The open structures obtained with the reaction scheme presented above and the KMC/MD code provide an explanation for the H/C ratios of soot precursors and young soots being greatly higher than those of polybenzenoid structures of equal molecular weight. Also, the curvature introduced by forming five- and six-membered rings is the most noticeable feature of these structures. The knowledge of the structures of soot precursor compounds is important to further progress with respect to the question about soot formation models by applying the KMC/MD code to follow the time evolution of a statistical ensemble of molecules, as well as the time evolution of extremely large molecules. Chemical characteristics like H/C [43], moieties measurable by nuclear magnetic resonance [44] and laser microprobe mass spectrometry [45] can be evaluated through a large number of simulations using the KMC/MD code. In addition, physical properties such as density and porosity [46] can be calculated from the chemical structure.

Simulations carried out to atomic mass units greater than 500 show the transition from two- to three-dimensional structures. Space limitations prelude presentation of these results.

Acknowledgment

This research is funded by the University of Utah Center for the Simulation of Accidental Fires and Explosions (C-SAFE), funded by the Department of Energy, Lawrence Livermore National Laboratory, under subcontract B341493. This work was performed under the auspices of the U.S. Department of Energy by University of California Lawrence Livermore National Laboratory under contract number W-7405-Eng-48.

REFERENCES

1. Graham, S. C., *Proc. R. Soc. London* A377:119 (1981).
2. Mauss, F., Trilken, B., Breitbach, H., and Peters, N., in *Soot Formation in Combustion: Mechanisms and Models* (H. Bockhorn, ed.), Springer-Verlag, Berlin, 1994, p. 325.
3. Böhm, H., Jander, H., and Tanke, D., *Proc. Combust. Inst.* 27:1605 (1998).
4. D'Anna, A., and Violi, A., *Proc. Combust. Inst.* 27:425 (1998).
5. Wornat, M. J., Sarofim, A. F., and Lafleur, A. L., *Proc. Combust. Inst.* 24:955 (1992).
6. Mukherjee, J., Sarofim, A. F., and Longwell, J. P., *Combust. Flame* 96:191 (1994).
7. Mulholland, J. A., Mukherjee, J., and Sarofim, A. F., *Energy Fuels* 11:392 (1997).
8. D'Anna, A., Violi, A., and D'Alessio, A., *Combust. Flame* 121:418–429 (2000).
9. Violi A., Truong T. N., and Sarofim A. F., *Combust. Flame* 126:1506 (2001).
10. D'Anna, A., Violi, A., D'Alessio, A., and Sarofim, A. F., *Combust. Flame* 127:1995 (2001).
11. Alder, B. J., and Wainwright, T. E., *J. Chem. Phys* 31:459 (1959).
12. Haile, J. M., *Molecular Dynamics Simulation: Elementary Methods*, Wiley, New York, 1992.
13. Westbrook, C. K., Kubota, A., and Pitz, W. J., *Computational Chemistry of Plasma Polymerization*, LLNL Laboratory Directed Research and Development FY 1999, Lawrence Livermore National Laboratory Annual Report, 1999, p. 4.
14. McDermott, J. B., Libanati, C., La Marca, C., and Klein, M. T., *Ind. Eng. Chem. Res.* 29(1):22 (1990).
15. Neurock, M. N., Nigam, A., Libanati, C., and Klein, M. T., *Chem. Eng. Sci.* 45(8):2083 (1990).
16. Zhigilei, L. V., and Garrison, B. J., *Appl. Phys. Lett.* 74(9):1341 (1999).
17. Brenner, D. W., *Phys. Rev. B* 42:9458 (1990).
18. Tersoff, J., *Phys. Rev. Lett.* 61:2879 (1988).
19. Gelten, R. J., Jansen, A. P. J., van Santen, R. A., Lukkien, J. J., Segers, J. P. L., and Hilbers, P. A. J., *J. Chem. Phys.* 108:5921 (1998).
20. Virtual Kinetic Laboratory, University of Utah, 2002, http://vklab.hec.utah.edu.
21. Zhang, S., and Truong, T. N., *J. Phys. Chem. A*, in press (2002).
22. Becke, A. D., *J. Chem. Phys.* 96:2155 (1992); 97:9173 (1992); 98:5648 (1993).
23. Lee, C., Yang, W., and Parr, R. G., *Phys. Rev. B* 37:785 (1988).
24. Hehre, W., Radom, L., Schleyer, P. R., and Pople, J. A., *Ab Initio Molecular Orbital Theory*, Wiley, New York, 1986.
25. Zhang, S., and Truong, T. N., *J. Phys. Chem. A* 104:7304 (2000).
26. Zhang, S., and Truong, T. N., *J. Phys. Chem. A* 105:2427 (2001).
27. Richter, H., Mazyar, O. A., Sumathi, R., Green, W. H., Howard, J. B., and Bozzelli, J. W., *J. Phys. Chem. A* 105:1561 (2001).
28. Frisch, M. J., Trucks, G. W., Schlegel, H. B., et al., *Gaussian 98, Revision A.7*, Gaussian Inc., Pittsburgh, PA, 1998.
29. Bittner, J. D., and Howard, J. B., in *Particulate Carbon: Formation during Combustion* (D. C. Siegla and G. W. Smith, eds.), Plenum Press, New York, 1981, p. 109.

30. Kee, R. J., Rupley, F. M., and Miller, J. A., *Chemkin II: A FORTRAN Chemical Kinetics Package for the Analysis of Gas Phase Chemical Kinetics*, Sandia report SAND 89-8009B.
31. Violi, A., D'Anna, A., and D'Alessio, A., *Environ. Combust. Technol.*, in press (2001).
32. Frenklach, M., Clary, D. W., Gardiner, W. C., and Stein, S. E., *Proc. Combust. Inst.* 20:887 (1984).
33. Benish, T. G., Lafleur, A. L., Taghizadeh, K., and Howard, J. B., *Proc. Combust. Inst.* 26:2319 (1996).
34. McEnally, C. S., and Pfefferle, L. D., *Combust. Sci. Technol.* 131:323 (1998).
35. Frenklach, M., and Ebert, L. B., *J. Phys. Chem.* 92:561 (1988).
36. Frenklach, M., Moriarty, N. W., and Brown, N. J., *Proc. Combust. Inst.* 27:1655 (1998).
37. Frenklach, M., *Proc. Combust. Inst.* 26:2285 (1996).
38. Mulholland, J. A., Lu, M., and Kim, D.-H., *Proc. Combust. Inst.* 28:2593 (2000).
39. Lafleur, A. L., Howard, J. B., Taghizadeh, K., Plummer, E. F., Scott, L. T., Neeula, A., and Swallow, K. C., *J. Phys. Chem.* 100:17421 (1996).
40. Evans, M. G., and Polanyi, M., *J. Chem. Soc. Faraday Trans.* 32:1340 (1936).
41. Violi, A., Sarofim, A. F., and Truong, T. N., in *Proceedings of* the *Second International Mediterranean Combustion Symposium* (M. Kamel and M. S. Mansour, eds.), Sharm El Sheik, Egypt, 2002, p. 1161.
42. Violi, A., Truong, T. N., and Sarofim, A. F., unpublished data.
43. Keller, A., Kovacs, R., and Homann, K.-H., *Phys. Chem. Chem. Phys.* 2:1667 (2000).
44. Solum, M. S., Sarofim, A. F., Pugmire, R. J., Fletcher, T. H., and Zhang, H., *Energy Fuels* 15:961 (2001).
45. Dobbins, R. A., Fletcher, R. A., and Chang, H.-C., *Combust. Flame* 115:285 (1998).
46. Acharya, M., Strano, M. S., Mathews, J. P., Billinge, S. J. L., Petkov, V., Subramoney, S., and Foley, H. C., *Phil. Mag. B* 79:1499 (1999).